NOVEL PLACEMENT OF SERPENTINE SPRING TO REDUCE PULL-IN VOLTAGE OF A MEMS BASED SWITCH

P. Rohit Nair[1], S. Gowtham[2], T. Avinash[3], Y. Saranya[4], Vijay Kumar[5], Virender Singh[6]*

Article History: **Received: 20.04.2023** **Revised: 26.05.2023** **Accepted: 13.06.2023**

Abstract:
In this work, a MEMS based capacitive switch is designed and analyzed for reduced pull-in voltage. The major flexures like cantilever and clamped-clamped structures are studied and it is found that serpentine spring produces lowest spring constant and therefore it is utilized in the design to make spring loaded proof mass. The designed switch consists of serpentine spring and proof mass to allow the displacement required for the electrostatic actuation. In the bottom of the proof-mass an air gap of five micrometer is kept a dielectric layer of thickness three micrometer is deposited and finally a metal layer of gold is deposited as a ground line. The material used for the proof mass is polysilicon. The variation in the Pull-in voltage is studied by changing dielectric layer thickness and with other dielectric materials also. The switch is simulated based on the FEM method to validate the design in terms of numerical simulations. The pull-in voltage and figure of merit is calculated theoretically and the compared with the simulated results. The simulation results ae in line with the analytical results.

Keywords: MEMS, FEM.

[1,2,3,4,6]*NS Raju Institute of Technology, Visakhapatnam-531173, India. [6]Email: nain_virender@yahoo.com
[5]Terminal Ballistic Research Laboratory, DRDO, Sector 30, Chandigarh-160030, India

***Corresponding Author:** Virender Singh
*NS Raju Institute of Technology, Visakhapatnam-531173, India. Email: nain_virender@yahoo.com

DOI: 10.48047/ecb/2023.12.si5a.0530

1. Introduction

Micro Electromechanical systems (MEMS) are the integrated micro devices or systems relating electrical and mechanical components developed by using Integrated Circuit (IC) which are usually compatible to batch-processing fabrication techniques ranging in size from micrometers to few millimeters. These systems are accomplished to have sensing and actuation at the micro level or acting like an additive sensor array to produce things at the macro scale. MEMS has been emerged as the state-of-the-art technology to produce sensors for different applications related to biological, chemical or any physical phenomenon. This technology sometimes permits to fabricate mechanical sensor and interface electronics on the same wafter. Even though MEMS technology emerges from IC fabrication techniques, test methods of both technologies significantly differ from each other. RF MEMS switches are one the important device which have been greatly discussed after the development of the MEMS based processes. They are used to perform 'ON' and 'OFF' like any switch but the main difference that theses switches use to facilitate the contact in the radio frequency range. RF Switches are mostly based on the capacitance change which is measure for 'OFF' and 'ON' stare differently. Therefore, capacitive coupling is mainly utilized in the working of RF MEMS switches. The primary parameter in RF switches is pull-in voltage which should be smaller after the optimization of other parameter like response time, current handling capabilities etc. A detailed review of RF MEMS switches is presented by taking into consideration the important features like actuation mechanism, design of mechanical flexure and the design of the contact mechanism by utilizing different spring-mass systems [1]. Usually capacitive type with clamped-clamped structure is utilized in the RF MEMS switches. The theoretical and numerical analysis of pull-in voltage is reported in 2015 [2], where figure-of-merit and pull-in voltage are optimized in the analysis of MEMS based RF switch. The effect on pull-in voltage due to different dielectric materials like Silicon Dioxide, Silicon Nitride, Aluminum Oxide, Tantalum Pentoxide and Titanium Dioxide is discussed in details. It is observed that aluminum oxide suit as the best dielectric material to improve figure-of-merit of the capacitive RF MEMS switch. The RF MEMS switch reported in [3], three different RF shunt MEMS switches are discussed and for Multiphysics simulation COMSOL software is used. The pull-in voltage and switching time study is reported in this work. After reviewing some of the previous works on the RF MEMS switches [4-14] it is observed that pull in voltage is the most essential parameter in the design of the RF MEMS switch and it is observed that many people are trying to design RF MEMS switch with lower pull-in voltage. In this work we have designed RF MEMS switch with a very low pull-in voltage compared to existing models it is achieved because the specific placement of the serpentine meanders at the end corners of the beam it is observed that the pull-in voltage in this switch is around(7-8V) which is very low compared to existing designs discussed above.

2. Proposed switch design

The proposed switch is a shunt capacitive switch with silicon substrate and mechanical structure of polysilicon due its excellent mechanical performance and access to advance to microelectronics processes. The optimized parameters for the switch are given in the table I. As shown in the figure 1, the proposed switch consists of a serpentine spring-mass system on the top and by following an air gap dielectric is placed along with the bottom electrode. The main interesting fact in the design perspective is the placement of the serpentine springs, it is a novel type of placement used first time in this particular configuration. The primary advantage of this configuration is that the motion of the proof-mass is constrained in the sensing direction only. Therefore, it will not go in other direction is the one advantage and other thing the ohmic contact will be proper with good contact area.

Table 1. Design Specifications of Switch Parameter

Parameter	Length (μ**m)**	Width (**μm)**	Thickness (**μm)**	Material
Substrate	500	400	5	SILICON
Electrode	500	400	1	GOLD
Dielectric	500	400	2	Al_2O_3
Sacrificial	2000	800	2	Si_3N_4
Structure	1000	800	5	POLYSILICON

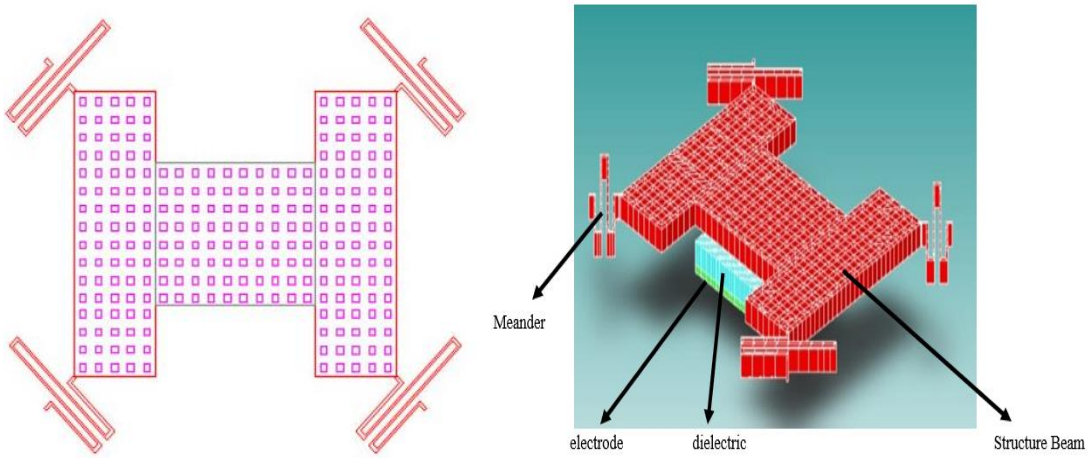

(a) (b)

Figure 1(a) Proposed switch 2D layout of the proposed switch 1(b) 3D model

3.1. Microcantilever

Spring constant is key factor for analysing mechanical behaviour of proposed switches. Spring constant k of the serpentine spring utilized in the proposed switch is given by equation (1) [15].

$$k = n_b \frac{Ewt^3}{l^3} \qquad (1)$$

Where E is the Young's modulus, t represents the thickness of the spring, L represents the length of the spring and n_b represents the number of meanders in the serpentine spring. The value of the spring constant is optimized on the basis of the above-mentioned parameters. The primary perspective in deciding spring constant is the targeted natural frequency of the spring-mass system which is the primary source of the mechanical displacement. Therefore, all the parameters are optimized to get the desired value of the spring constant shown in the figure 2.

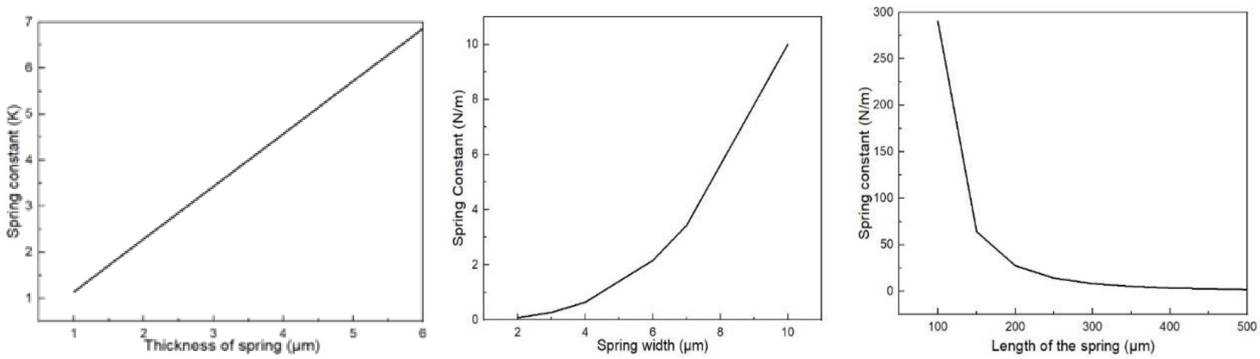

(a) (b) (c)

Figure 2. (a) Spring constant vs thickness (b) Spring constant vs width (c) Spring constant vs length

Figure 2(a) shows the variation of the spring constant with the thickness of the serpentine spring, it is clear that variation is linear. Therefore, a value of the thickness can be selected based on the fabrication limitations of the foundry. Figure 2(b) shows the variation with the width of the serpentine spring and it is clear that relationship is non-linear. Therefore, width of the serpentine spring play's major role in deciding the spring constant and selection of the thickness depends on the limitation of the fabrication processes and second is the requirement of the spring constant. Figure 2(c) shows the variation of the spring constant with the length of the spring and this length of the spring should be less so that design space can be minimized. Overall, these all three parameters of selecting spring constant depends on the available design space, targeted natural frequency and the fabrication limitations. The optimized parameter for serpentine spring i.e., length, breadth, width is 400µm, 7µm and 5µm respectively.

3. Results and analysis

3.1. Modal analysis

The primary design property of the switch is the natural frequency which decide the maximum permitted mechanical displacement for a given load. The mechanical displacement of the single degree of freedom system is magnitude of the input load, duration of the input load and the natural time period or natural frequency of the responding structure [19]. Therefore, it becomes very important to select natural frequency of the switch. In the proposed design our aim is to allow this spring-mass system to displace under the influence of electrostatic force only in one direction i.e., toward bottom electrode, in all other direction it should be less sensitive. In order to realize this, we are proposing a novel placement of the serpentine spring with the proof-mass to facilitate only unidirectional motion under the influence of the electrostatic force. Therefore, modal analysis becomes very important in this case and in this work, we have simulated the switch to find about the natural modes of this switch. Table 2, listed the value of natural frequency for first six modes and the corresponding modes shapes is shown in the figure 3. It can be observed that the first natural mode of the designed switch is allowing mode displacement towards the bottom electrode only and the value of natural frequency is 2.23 kHz, therefore the switch is more sensitive in this direction only.

Table 2. Simulated results of Frequency of modes

Sr. No.	Frequency (kHz)
1	2.23058
2	3.86115
3	5.028559
4	15.17949
5	15.82281
6	15.92871

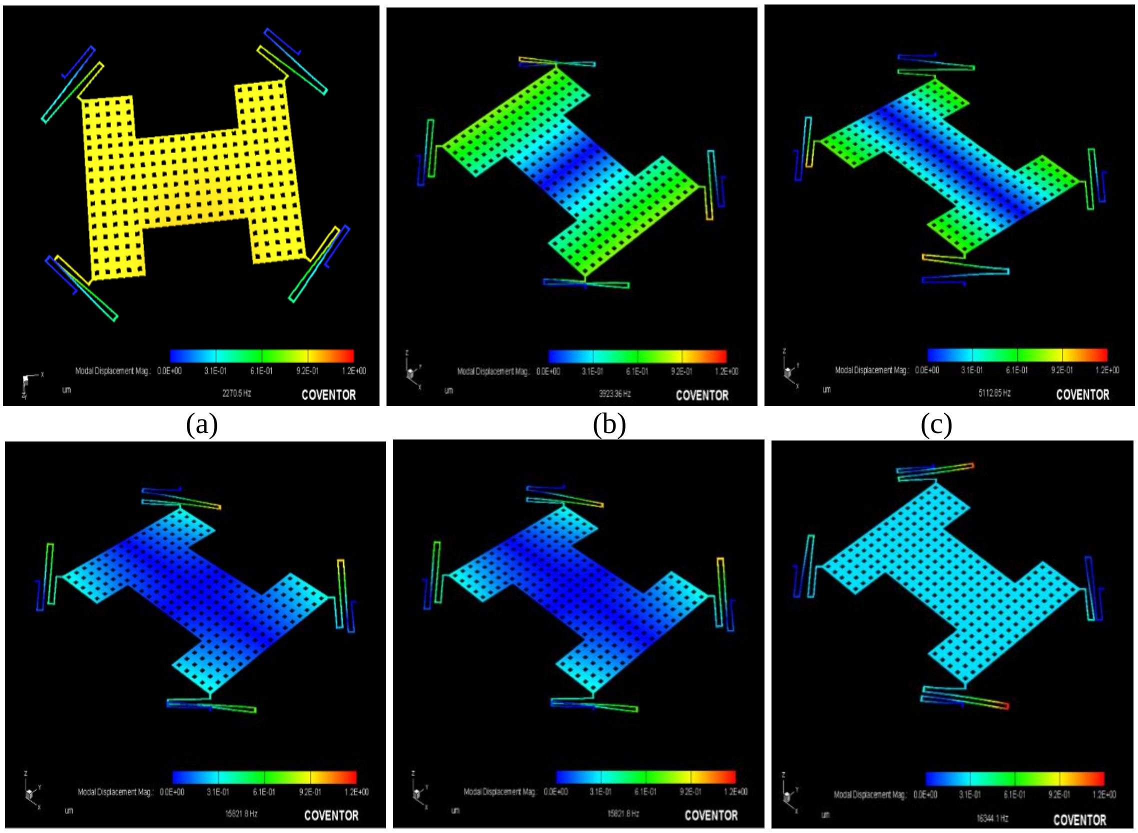

(a) (b) (c) (d) (e) (f)

Figure 3 (a) First mode (b) Second Mode (c) Third mode (d) Fourth mode (e) Fifth mode (f) Sixth mode

3.2. Pull-in voltage and simulation

After selecting the natural frequency second important parameter in the design process of switch is the pull-in voltage. It is the minimum applied voltage applied between two electrodes after which the actuation happens under the influence of the electrostatic force. During the optimization process, researchers are focusing to reduce the pull-in voltage. The analytical formula for the pull-in voltage is given by V_p equation (2) [2].

$$V_p = \sqrt{\frac{8\,k\,d^3}{27\,\mathcal{E}_0 \mathcal{E}_a A_p}} \quad (2)$$

Where k represents spring constant, $\mathcal{E}_0$ is the relative permittivity of the air, $\mathcal{E}_a$ represents the relative permittivity of the dielectric material, d is the initial gap between electrode and A_p is the area of the contact electrode. By varying these parameters pull-in voltage can be calculated and since low pull-in voltage is the primary target and the above-mentioned parameters can be optimized for the pull-in voltage. The variation of the pull-in voltage with these parameters is shown in the figure 4.

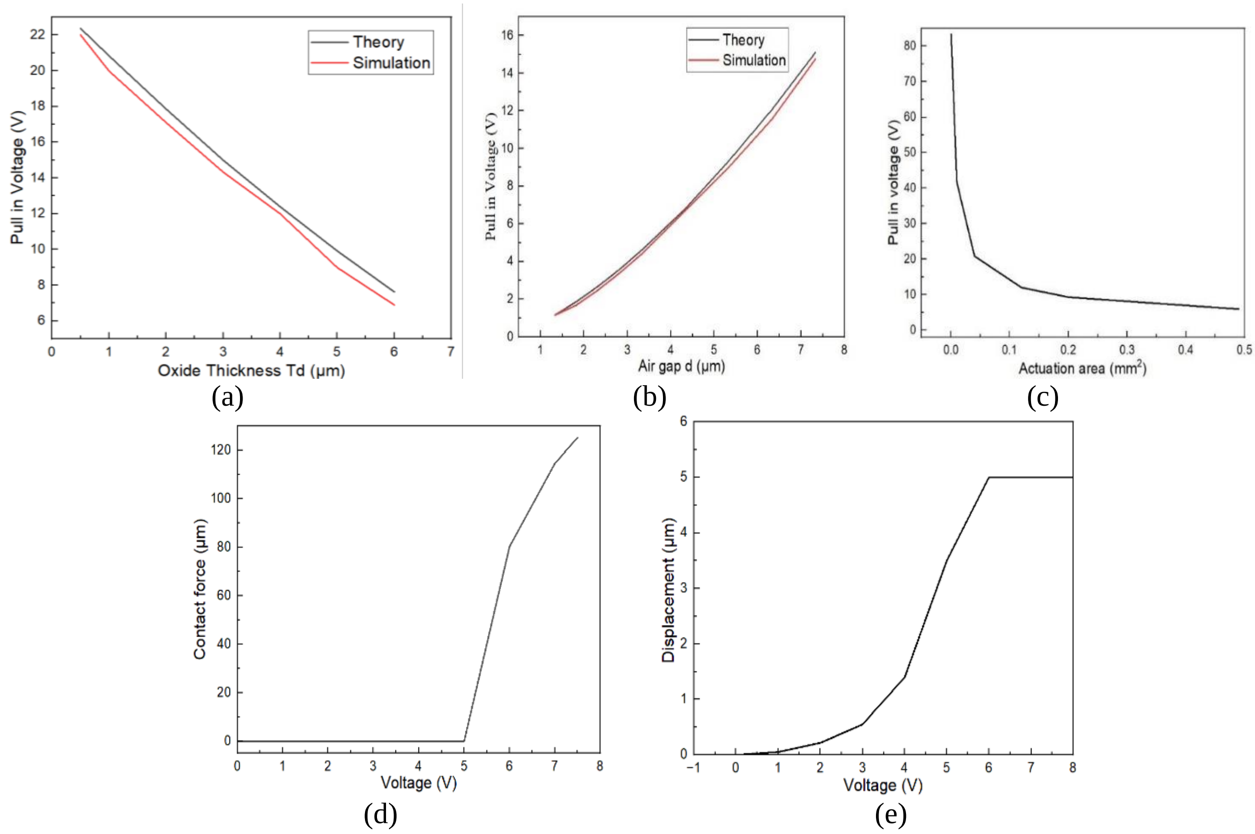

Figure 4. (a) Pull-in voltage vs dielectric thickness (b) pull-in voltage vs air gap (c) pull-in voltage vs actuation area (d) pull-in voltage vs contact force (e) pull-in voltage vs displacement.

In the figure 4(a), the variation between pull-in voltage and thickness of the dielectric layer. It is observed that pull-in voltage is decreasing with the increase of the oxide thickness and both analytical and simulated results are matching with each other. In figure 4(b), the variation of the pull-in voltage with air gap between the dielectric and the proof-mass by keeping thickness of the dielectric to 3µm. It is observed that both theoretical and simulation value are matching with each other and the pull-in value is increasing with the increase in the gap. The pull-in voltage varies exponentially with the actuation area, as shown the figure 4(c). The value of the actuation area should be large enough to reduce pull-in voltage but at the same time the value of the actuation area should be as per design space utility. It can be observed that after pull-in voltage the contact is happening and the value of the contact force is above 100 µN which can be considered good for the ohmic contact analysis. The variation of the pull-in voltage and contact force is shown in the figure 4(d). The simulated displacement response of the top electrode with the voltage as shown in the fig 4(e). It can be observed in the graph that displacement starts increasing with the increase of the applied voltage, as the proof-mass travel 5µm gap then contact formation is there. Therefore, after achieving the pull-in voltage further displacement is restricted due the contact with the bottom part. The contour plot of the displacement is shown in the figure 5(a) and it can be observed that the proof-mass is having the maximum displacement. Mises stresses are useful in predicting the reliability of the switch and the contour plot for stress is given by figure 5(b). For this design the maximum value of the mises stress is 20MPa observed in the serpentine spring which is far away from the ultimate tensile strength which is around 7000MPa. Therefore, this design is robust in terms of mechanical reliability. In this design the obtained values of stress around 20MPa (mega pascals) and the stress on the silicon is around 7000MPa where there is so much different and very large gap in between stresses obtained. The values of the stress can be seen in bottom the contour plot by observing colours upon the switch it is proven that the switch design has very less stress compared to other switch design that are already existed.

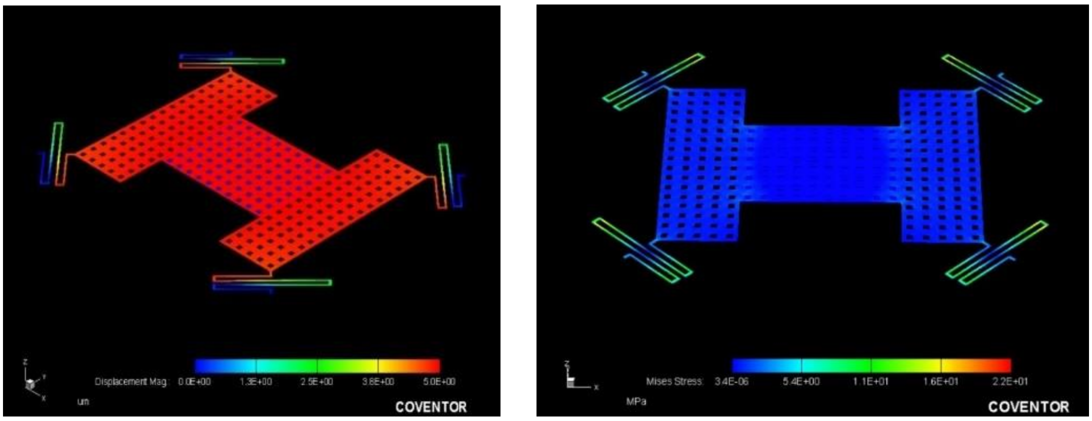

(a) (b)

Figure 5. Simulated (a) Displacement contour plot (2) stress contour plot.

3.3. Capacitance Ratio

The capacitance between the top and bottom electrode of the switch when no input voltage is applied is termed as the off-state capacitance represented by C_{off} is given by equation (3). Whereas when a voltage greater than the pull-in voltage is applied between top and bottom electrode of the switch then the measured capacitance is called on-state capacitance (C_{on}) given by equation (4) [2]. Where each terms have their usual meaning.

$$C_{off} = \frac{\mathcal{E}_0 A_p}{G + T_d(\frac{2}{\mathcal{E}_d} - 1)} \quad (3)$$

$$C_{on} = \frac{\mathcal{E}_0 \mathcal{E}_d A_p}{T_d} \quad (4)$$

Therefore, the figure of merit (C_r) can be calculated by the ratio of on-state capacitance to the off-state capacitance and given by equation (5).

$$C_r = \frac{C_{on}}{C_{off}} \quad (5)$$

Thus, after putting all the design values into the equation (3), (4) and (5), the figure of merit is 135 which indicates great isolation between on-state and the off-state. The results of the current work are compared with the existing work is tabulated in the table 3. It is evident that by using this novel design of the MEMS based switch have the low pull-in voltage in comparison to the existing switches [9,10, 12-13].

Table 3. comparison table between existing work and proposed work

Parameter	Ref. [19]	Ref. 20	Ref. [21]	Ref. [3]	Proposed switch
Pull-in voltage	50V	20.4 V	20.4 V	16.9 V	9.33 V
Stress analysis	-	-	-	1.286 MPa	20 MPa
Up state capacitance	-	137 fF	137 fF	7.46 fF	4.72fF
Down state capacitance	-	3.9 pF	3.9 pF	1.25 pF	3.49pF
Capacitance ratio	-	-	-	16.75	135.33

5. Conclusion

This work presented a MEMS based switch with the reduced pull-in voltage. A novel geometrical design of serpentine spring with proof mass is taken for this switch. This design allows proof mass to move in singe direction only i.e., in the sense direction. Therefore, pull-in voltage becomes very low for this. Further the figure of merit is calculated by taking the ratio of the on-state capacitance to the off-state capacitance which is 136. analysis of effect of dielectric layer thickness in order to reduce the pull-in-voltage and increase the capacitance ratio value using materials such as Silicon Dioxide, Silicon Nitride, Aluminium Oxide, Tantalum Pentoxide and Titanium Dioxide.

6. Data Availability Statement

All the simulation data which is used in the manuscript is present with the corresponding author.

References

1. Kurmendra and Rajesh Kumar, "RF micro-electro-mechanical system (MEMS) capacitive switch performance parameters and improvement strategies", Microsystem Technologies Volume 28 Issue 8 Aug 2022 pp 1765–1783.
2. Rajesh Saha, Santanu Maity, Ngasepam Monica Devi, and Chandan Tilak Bhunia, "Analysis of Pull-in-Voltage and Figure-of-Merit of Capacitive MEMS Switch" Transactions on Electrical and Electronic Materials Vol. 17, No. 3, pp. 129-133, June 25, 2016
3. S Girish Gandhi, I Govardhani, M Venkata Narayana and K Sarat Kumar, "Performance Comparison of Shunt Rf Mems Switches", Turkish Journal of Computer and Mathematics Education (TURCOMAT), Vol. 12 No. 5 (2021).
4. Mamleyev, E.R.; Lee, C.H.; Korvink, J.G.; Kohl, M.; Poletkin, K.V. Experimental Study and Simulation of Pull-In Behavior in Hybrid Levitation Microactuator for Square-Shaped Proof Masses. *Actuators* **2023**, *12*, 48.
5. Devakirubai, E.E., Kannan, S. & Manivannan, M. Design and performance analysis of a dual channel RF MEMS switch with separate bias voltage and signal paths for aerospace applications. Int J Interact Des Manuf (2023).
6. Yang, X.; Kästner, P.; Käkel, E.; Smolarczyk, M.; Liu, S.; Li, Q.; Hillmer, H. Study of Dynamics in Metallic MEMS Cantilevers—Pull-In Voltage and Actuation Speed. *Appl. Sci.* **2023**, *13*, 1118.
7. Z. Ma *et al*., "Pull-In Dynamics of Two MEMS Parallel-Plate Structures for Acceleration Measurement," in *IEEE Sensors Journal*, vol. 21, no. 16, pp. 17686-17694, 15 Aug.15, 2021.
8. Piotr Skrzypacz, Shirali Kadyrov, Daulet Nurakhmetov, Dongming Wei, "Analysis of dynamic pull-in voltage of a graphene MEMS model", Nonlinear Analysis: Real World Applications, Volume 45, 2019, Pages 581-589, ISSN 1468-1218.
9. K. Girija Sravani *et al*., "Design and Performance Analysis of Low Pull-In Voltage of Dimple Type Capacitive RF MEMS Shunt Switch for Ka-Band," in *IEEE Access*, vol. 7, pp. 44471-44488, 2019.
10. T. Singh, N. K. Khaira and R. R. Mansour, "Thermally Actuated SOI RF MEMS-Based Fully Integrated Passive Reflective-Type Analog Phase Shifter for mm Wave Applications," in *IEEE Transactions on Micro wave Theory and Techniques*, vol. 69, no. 1, pp. 119-131, Jan. 2021.
11. Ajay Sudhir Bale, Suhaas V. Reddy, Shivashankar A. Huddar, Electromechanical characterization of Nitinol based RF MEMS switch, Materials Today: Proceedings, Volume 27, Part 1, 2020,Pages 443-445, ISSN 2214-7853.
12. G. Zorpette, "RF MEMS deliver the "ideal switch": After two decades of development, MEMS-based RF switches are finally finding real-world uses," in *IEEE Spectrum*, vol. 57, no. 8, pp. 8-9, Aug. 2020.
13. H Busta, R Amantea, D Furst, J M Chen, M Turowski and C Mueller, "A MEMS shield structure for controlling pull-in forces and obtaining increased pull-in voltages", J. Micromech. Microeng. 11 720, 2001.
14. Michael Gomez, Derek E Moulton and Dominic Vella, "Delayed pull-in transitions in overdamped MEMS devices", J. Micromech. Microeng. 28 015006, 2018.
15. G. K. Fedder, "Simulation of Micro Electro Mechanical systems," Ph.D. dissertation, Dept. Elect. Eng., Comput. Sci., UC Berkeley, Berkeley, CA, USA, 1994.
16. Giridhar MS, Jambhalikar A, John J, Islam R, Nagendra CL, Alex TK, "An X band RF MEMS switch based on silicon-on-glass architecture", Sadhana, vol:34 (4), pp: 625-628, (2009).
17. Mafinejad Y, Kouzani A, Mafinezhad K, Hossein nezhad R, "Low insertion loss and high isolation capacitive RF MEMS switch with low pull-in voltage", The International Journal of Advanced Manufacturing Technology, vol. 93, pp: 661-670, (2017)
18. M Tang, A.B Yu, A.Q Liu, A. Agarwal, S. Aditya, Z.S Liu, "High Isolation X-band MEMS Capacitive Switches", Elsevier, vol. 120, pp. 95-98, (2005).
19. C.M. Harris, A.G. Piersol and T.L. Paez, "Shock and Vibration Handbook," McGraw-Hill, (1961). ISBN: 9780071508193.